H06

Search for Thermal X-ray Features from the Crab Nebula with Hitomi SXS

M. Tsujimoto[1], K. Mori[2], S-H. Lee[3,4], H. Yamaguchi[5], N. Tominaga[6,7], T. J. Moriya[8], T. Sato[9], A. Bamba[10], Hitomi Collaboration

[1]JAXA ISAS, [2]Miyazaki U., [3]Kyoto U. [4]RIKEN, [5]NASA GSFC, [6]Konan U., [7]U. of Tokyo IPMU, [8]NAOJ, [9]TMU, [10]U of Tokyo

<tsujimot@astro.isas.jaxa.jp> (MT) <mori@astro.miyazaki-u.ac.jp> (KM)

1. SUMMARY

The Crab nebula originated from a core-collapse SN explosion observed in 1054AD. When viewed as an SNR, it has an anomalously low observed ejecta mass[1] and kinetic energy[2,3] for an Fe-core collapse SN. Intensive searches were made for a massive shell[4] that solves this discrepancy, but none has been detected[5-9]. An alternative idea is that the SN 1054 is an electron-capture (EC) explosion[10] with a lower explosion energy by an order of magnitude than Fe-core collapse SNe.

In the X-rays, imaging searches were performed for the plasma emission from the shell in the Crab outskirts to set a stringent upper limit to the X-ray emitting mass[9]. However, the extreme brightness of the pulsar wind nebula hampers access to its vicinity. We thus employed spectroscopic technique using the X-ray micro-calorimeter[11] onboard the Hitomi satellite[12].

By exploiting its superb energy resolution (Fig 1), we set an upper limit for emission or absorption features from yet undetected thermal plasma in the 2–12 keV range. We also re-evaluated the existing Chandra[9] and XMM-Newton[13] data. By assembling these results, a new upper limit was obtained for the X-ray plasma mass of ~1 Mo for a wide range of assumed shell radius, size, and plasma temperature both in and out of the collisional equilibrium.

To compare with the observation, we performed HD simulations of the Crab SNR for two SN models (Fe-core vs EC scenario) under two SN environments (uniform ISM vs progenitor wind). We found that the observed mass limit is compatible with both SN models if the environment has a low density of <0.03 cm^{-3} (Fe core) or <0.1 cm^{-3} (EC) for the uniform density, or a wind density smaller by a factor than the wind of a mass loss rate=10^{-5} Mo/yr and a velocity=20 km/s for the wind environment.

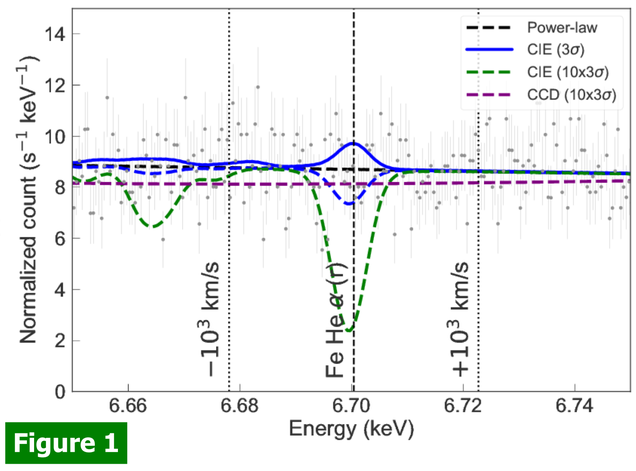

Figure 1

Power of a high-resolution, non-dispersive spectrometer for weak lines from extended sources. Blue curves are Fe He-α line detectable with SXS spectrum (grey) at 3σ. Green is x10 of blue. Purple is a mock CCD spectrum of green, which is indistinguishable from the continuum.

2. OBSERVATIONS

The Crab was observed for 10 ks on 2016 March 25. Due to unfinished instrumental set-up, sensitivity at ~0.1-2 keV was not achieved.

Due to the high count rate, some pixels at the 6x6 array center suffer dead time. Still, the observing efficiency of ~72% for the entire array is much higher than conventional CCD X-ray spectrometers. For example, Suzaku XIS requires a 1/4 window + 0.1 s burst clocking mode to avoid pile-up for the same flux source, and the efficiency is only ~5%.

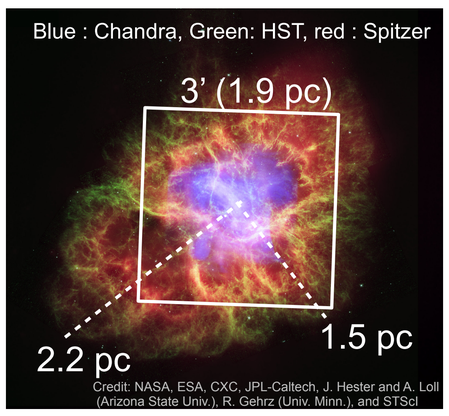

Figure 2

Three-color composite image of the Crab nebula and SXS field. This turned out to be the last data set of SXS.

3. ANALYSIS

3-1. Plasma Search

i) Emission (CIE): We used the apec model[14] for the CIE plasma, in which the electron, ion, and ionization temperatures are the same. Neither the bulk motion nor the turbulence broadening was considered, but the thermal broadening was taken into account for the lines. For each varying electron temperature (0.1-10 keV), we selected the strongest emission line in the 10 non-overlapping 1 keV ranges in the 2–12 keV band. For each selected line, we first fitted the ± 50 eV range around the line with a power-law model, then added the plasma emission model to set the upper limit of the volume emission measure (Y) of the plasma (Fig 3).

ii) Emission (NEI): We used the nei model[15], which calculates the collisional ionization as a function of the ionization age ($n_e t$), and accounts for the difference between the ionization and electron temperatures. We took the same procedure with the CIE plasma for log($n_e t$ cm^{-3} s)=10.0-13.5, and derived the upper limit of Y.

iii) Emission (Broadening): We considered the case that the electron and ion temperatures are different. More massive ions are expected to have a higher temperature than less massive ions and electrons, hence are more thermally broadened before reaching equilibrium. We derived the upper limit of Y for several values of the ion's thermal velocity v_i/c=0.001, 0.002, 0.005, 0.01, 0.02.

iv) Absorption: A similar procedure was taken for deriving the upper limit of the absorption column ($N_H^{(hot)}$) by a thermal CIE plasma. We used the hotabs model[15].

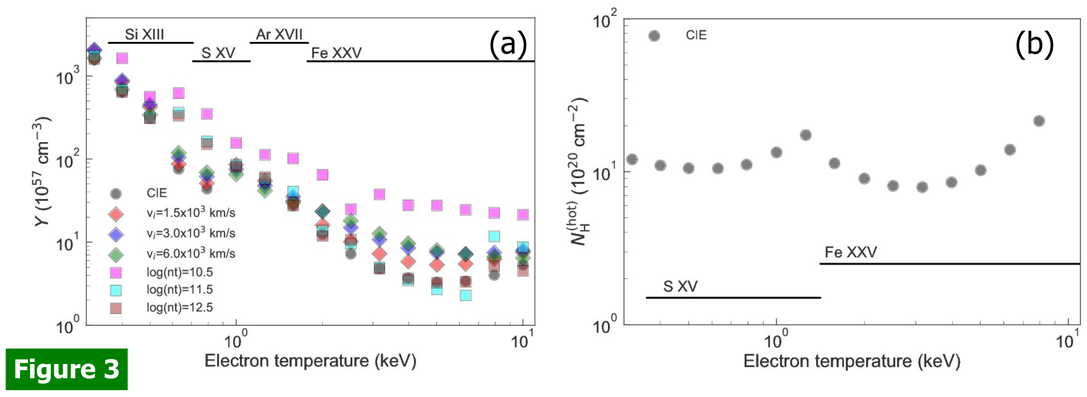

Figure 3

3σ statistical upper limit of (a) emission measure by emission search (i-iii) and (b) absorption column by absorption search (iv). The name of ions used for the limit is given at each Te.

3-2. Blind Search

We searched for emission or absorption line features at an arbitrary line energy in the 2–12 keV range. We made trials at 20,000 energies separated by 0.5 eV. The trials were repeated for a fixed line width corresponding to a velocity of v = 0, 20, 40, 80, 160, 320, 640, and 1280 km/s. For each set of line energy and width, we fitted and fixed the spectrum with a power-law model locally, and added a Gaussian model allowing both positive and negative amplitudes respectively for emission and absorption lines. No convincing line was detected.

4. DISCUSSION

4-1. Constraints on the plasma mass

For converting the upper limits of Y and $N_H^{(hot)}$ of the thermal plasma into that of the X-ray emitting plasma mass (M_X), we assumed that the plasma is uniform in a spherically symmetric shell in a range of R to R+ΔR from the center. Several shell fraction (ΔR/R) values were considered. We also re-evaluated the results by Chandra ACIS imaging[9] & XMM-Newton RGS spectroscopic[13] searches under the same assumptions. The most stringent limit is given by the emission search either by ACIS or SXS. The SXS result complements the ACIS result at R<1.3 pc, and the two give an upper limit of ~1 M ⊙ for the X-ray emitting plasma at any shell radius (Fig 4a).

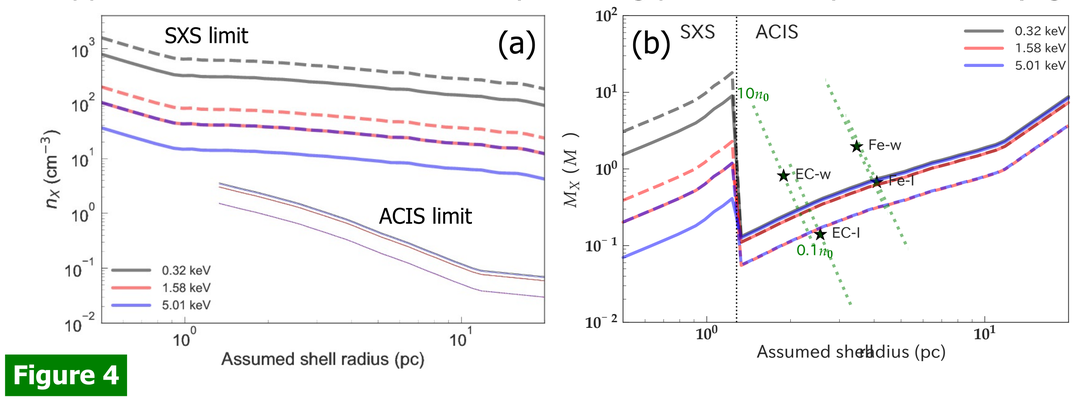

Figure 4

Upper limit of X-ray emitting plasma (a) density and (b) mass by SXS and ACIS for selected assumed plasma temperature (solid for CIE, dashed for $10^{10.5}$ s cm^{-3} NEI). Shell fraction of ⊿R/R=0.05 is assumed. In (b), HD simulation results are shown for 2x2 SN models, and their change of direction when the density changes by x0.1 or x10.

4-2. HD calculation & Comparison with observed limit

We performed a HD calculation to verify that the searched parameter ranges are reasonable and to confirm if any SN models are consistent with the observed limit. We used the CR-hydro-NEI code[17]. We considered (two SN explosion models **[Fe, EC]**) x (two circumstellar environments **[I, w]**). The former two are **[Fe]** the Fe-core collapse SN by a red super-giant progenitor with the initial explosion energy $E_0=1.21\times10^{51}$ erg and the ejecta mass M_{ej}=12.1 Mo[18], and **[EC]** the electron capture SN by a super AGB progenitor with $E_0=0.15\times10^{51}$ erg and M_{ej}=4.36 Mo[19]. The latter two are **[I]** the uniform density n_0=0.1 cm^{-3} and **[w]** the progenitor wind profile: $n_0(r)=dM_{wind}/dt/(4\pi v_{wind} m_p r^2)$, where $dM_{wind}/dt=1\times10^{-5}$Mo/yr and v_{wind}=20 km/s[19].

We compare the HD results with the observation (Fig 4b). We argue that both the Fe and EC models still hold to be compatible with the observed mass limits. In either case, it is strongly preferred that the pre-explosion environment is low in density; n_0<0.1 cm^{-3} (**EC-I**) or <0.03 cm^{-3} (**Fe-I**) for the ISM env, or $(dM_{wind}/dt)/v_{wind}<10^{14}$ g cm^{-1} for the wind env (both **Fe-w** and **EC-w**). For the latter, a large value (6×10^{18} g cm^{-1}) to explain the initial brightness of SN 1054[20] is not favored. Such a low density env is suggested by observations. At Crab, which is off-plane in the anti-Galactic center direction, the ISM density is ~0.3 cm^{-3} by a Galactic model[21]. The presence of a bubble is claimed around the Crab with a density lower than the surroundings[22].

References

[1] Fesen, R. A.+ (1997), AJ, 113, 354
[2] Davidson, K.+ (1985), ARA&A, 23
[3] Sollerman, J.+ (2000), ApJ, 537, 861
[4] Chevalier, R. A. (1977), Ap&& Library, 66, 53
[5] Frail, D. A.+ (1995), ApJL, 454, 129
[6] Tziamtzis, A.+ (2009), A&A, 474, 167
[7] Mauche, C. W.+ 1985
[8] Predehl, P.+ (1995), A&A, 293, 889
[9] Seward, F. D.+ (2006), ApJ, 652, 1277
[10] Nomoto, K.+ (1982), Nature, 299, 803
[11] Kelley, R. L.,+ (2016), Proc. SPIE, 9905
[12] Takahashi, T.+ (2016), Proc. SPIE, 9905
[13] Kaastra, J. S.+ (2009), A&A, 497, 291
[14] Smith, R. K.+ (2001), ApJL, 556, L91
[15] Smith, R. K.+ (2010), ApJ, 718, 583
[16] Kallman, T.+ (2001), ApJS, 133, 221
[17] Lee, S.-H.+ (2014), ApJ, 791, 97
[18] Patnaude, D. J.+ (2015), ApJ, 803, 101
[19] Moriya, T. J.+ (2014), A&A, 569, A57
[20] Smith, N. (2013), MNRAS, 434, 102
[21] Ferriere, K. (1998), ApJ, 497, 754
[22] Wallace, B. J.+ (1999), ApJS, 124, 181

"The X-ray Universe 2017" in Rome, Italy (June 6–9, 2017)